Cartography-oriented visual design of hydrodynamic ocean-physics datasets

Brad W. Robertson[1], Steffen D. Frey[1], Christian Kehl[1,*]

[1] Rijksuniversiteit Groningen, Bernoulli Institute, 9747 AG Groningen, The Netherlands
(s.d.frey, c.kehl)@rug.nl ; b.robertson@student.rug.nl

Keywords: Cartographic Design, Geo-Visualization, Oceanography, Hydrodynamic Fields, Visual Style Guide

Abstract

Oceanographic data and their related simulations have a key role in addressing EU and UN societal challenges in marine environments. Visualising marine data is challenging for different visual-communication intents and audiences, despite existing guidelines on the subject. A main visual-design limitation for existing techniques is the co-visualisation of multiple hydrodynamic field attributes in an accessible, comprehensible and engaging manner. This paper addresses this limitation in two ways: firstly, existing techniques for cartographic-oriented design of waterlines are adopted and extended towards multivariate hydrodynamic field datasets. Secondly, experimental results on the intermixing of different visual-channel mappings for hydrodynamic attribute data are presented in a case study on ocean-flow patterns around the Hebrides island chain (United Kingdom). The results demonstrate a comprehensible simultaneous co-visualisation of up to five unique, independent scalar attributes within a single-figure layout while preserving the geographic context. Moreover, insights and best-practices are stated in conclusion of the experimental case study to help oceanographic practitioners adopt the presented technology in their professional workflows.

1. Introduction

Processing, simulating and analysing hydrodynamic data are key activities in addressing EU missions and UN sustainability goals[1], such as climate-change adaptation and resilience, the conservation of the oceans and marine ecosystems, and the sustainable use of water resources. However, the value and impact of the data analysis are manifested when the data are visualised and discussed with the relevant stakeholders. At this stage, an effective visual design is needed to communicate the computational results in a comprehensible, summative way. Here, the visual design has to adapt to different audiences and communication intents (Munzner, 2014), highlighted by the following three examples. Firstly, public engagement is improved through aesthetic design aspects. Secondly, science workshop discussions can rely on prior domain knowledge of the audience when visually analysing multivariate attribute relations. Lastly, communicating multi-annual anomalies and trends to policy makers benefits from consistency and incremental approaches to the visual composition. Thus, stylistic flexibility is as important for marine visualisation techniques as a modular approach to the visual mapping of multivariate data.

This need is rarely met by existing flow-visualisation techniques, hydrodynamic field-plotting techniques, or photorealistic ocean-rendering approaches. Programmable plotting interfaces, such as matplotlib and pyplot (Hunter, 2007), are widely adopted in the ocean-science community, yet the provided plotting functions are limited in their customisation and composition flexibility. These limitations have recently been surveyed and analysed (Kehl et al., 2021), and perceptual colour maps were introduced (Kehl et al., 2022) in response to it. However, recent discussion panels at the Parcels anniversary workshop point out the more complex interpretability of these colour maps. Alternative flow-visualisation techniques are affected by similar drawbacks: finite-time Lyapunov exponent (FTLE) and finite-size Lyapunov exponent (FSLE) visualisation (Haller and Poje, 1998, Shadden et al., 2005) require the selection of adequate divergent colour maps to aid interpretability, whereas quiver plots quickly obfuscate emerging flow patterns in dense data regions (Kehl et al., 2022). Photorealistic ocean rendering, as technically demonstrated in computer graphics (Gutierrez et al., 2008, Shi et al., 2012) and recently implemented in popular-science outreach setups (Steenbeek et al., 2021, Fauville et al., 2024), often catches attention and short-term engagement from the audience. However, the technique is limited in terms of attribute modulation and visual mapping when presenting multivariate flow data. When plotting multiple relevant attributes, researchers often revert to multi-panel figures (i.e. a form of juxtaposition), which make insufficient use of the printed space while disassociating interlinked flow indicators.

In response to this gap, we investigate the rejuvenation of Cartography-oriented Design (CoD) (Semmo et al., 2015) as a visual style and an approach to map (i.e. *encode*) hydrodynamic data attributes to visualisation channels following the common visualisation pipeline (Chi, 2000). CoD is a category of visualisation techniques that replicate handcrafted cartographic stylization in a computerised, graphical, and mathematically-consistent way (Häberling et al., 2008). Amongst the cartographic styles for different application scenarios, such as terrain topography (Medyńska-Gulij, 2022), urban maps (Semmo et al., 2015), and transport networks (Trapp et al., 2015), the waterline stylisation by (Semmo et al., 2013) is taken as the basis for this work. The comparison baseline of the achieved results are traditional multi-panel figures of conventional colour maps. Our technical contribution in this respect is three-fold: (a) the identification of individual visual channels within this technique, (b) the extension of the base technique through *tufts*, *Bézier hatches* and automatic *compass-rose* placement, and (c) the actual mapping of hydrodynamic attributes to visual channels, resulting in several unique visualisations. Experiments using the new map style are then presented in a hydrodynamic case study of the Atlantic European North-West Shelf (ENWS) and scored according to the PREVis readability criteria. Based on these experiments, we derive application insights for practi-

* Corresponding author

[1] UN Sustainability Goals - `https://sdgs.un.org/goals`

tioners who aim to adopt the presented technique, which is our geospatial research contribution.

2. Related work

The primary goal of this research is to improve the visual communication of marine datasets in different visualisation settings. In the visualisation community, there are four widely-accepted key aspects that drive a visual design: *data, task, intent and audience* (Munzner, 2009, Munzner, 2014). While the *data* aspect is fixed on 2D hydrodynamic fields and the *tasks* are predefined per case, the visualisations need to adapt to different audiences and communication intents. This flexibility is expressed in the visualisation pipeline at the *mapping* stage, where different visual encodings can be applied to the same data, each using the same technique to create distinct visualisations that are tailored to the target audience and intent. That said, the selected visualisation technique is the limiting factor in terms of how many visual channels can be independently controlled to generate unique representations.

The selection of a flexible mapping technique is strongly inspired by historical nautical charts. This classical type of cartographic maps is accessible to both geo-technical audiences and domain experts within the marine and ocean sciences. The maps convey relevant attributes of marine navigation through elements such as numeric key information labels (e.g. depth or line orientation), landmark icons of significant points, contour indicators for coastal distances, one or more circular orientation indicators (e.g. compass-rose decorators), a distance scale, a thematic background colour and coloured key area contours (e.g. basin delineations). These visual elements are illustrated in fig. 1, and they can be adopted and expanded in order to create a digitally-analogous process to historical nautical mapping for modern hydrodynamic field data.

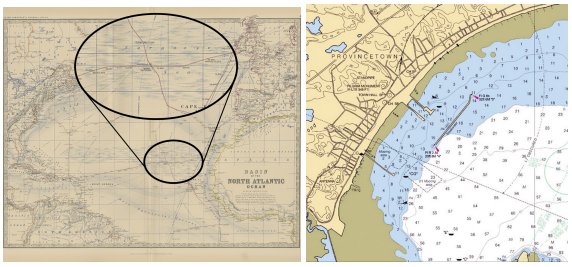

Figure 1. Illustration of historical nautical chart of the North Atlantic (left) and Provincetown, MA, USA (right). Key features are straight line strokes for distance measurements, depth map contours (right), written depth-markers (right), and flow hatches (left). Features such as radial compass indicators and relative-distance indicators are also common in nautical charts.

The main technical inspiration for modulating and implementing the nautical map style is the cartographic stylisation of water surfaces (Semmo et al., 2013). In this paper, the authors replicate historical map representations of rivers and coastal areas through a distance transform of the masked water area within a region. The continuous Euclidean distance transform facilitates the placement of lines, line segments, or texture-sampled hatching patterns within the water area at isotropic or anisotropic distances from coastlines. This enables the replication of historical map styles for water surfaces using non-photorealistic rendering (NPR). Yet, only one physical parameter is used for the graphical modulation, namely the coastline distance. Other artistic and parametrisable water representations include texture-based flow visualisations and noise-texture approaches (Van Wijk, 2002, Zhang et al., 2016), as well as a depth-based re-colourisation of coastal maps with handcrafted or standardised colour palettes (Masse and Christophe, 2015, Masse and Christophe, 2016). That said, both approaches are not suitable for this case: the re-colourisation only works as modulator for a single scalar parameter, and the image-based flow visualisation relies on Lagrangian particle simulations for creating the noise patterns. This latter case is not compatible with the Eulerian field input data.

3. Methodology

This section first clarifies the data layout, its dimensions, and the target attributes available for visual modulation. Next, we discuss our hydrodynamic visualisation using a contour-based cartographic stylisation technique. Lastly, we demonstrate the visual encoding methods available via this new technique.

3.1 Hydrodynamic ocean data

Hydrodynamic ocean field data are stored as rectilinear or curvilinear staggered Arakawa grids (Arakawa and Lamb, 1977). Each grid cell stores multiple scalar, vector, or tensor attributes. The grid coordinates predominantly use either the WGS84 coordinate system (EPSG:4326; EPSG:4978) or metric UTM (x, y, z) triplets. We exclude the depth-related data dimension, focusing on the 2D lateral visualisation case.

Hydrodynamic datasets include fluid-flow velocities and their associated biophysical tracers as output of Eulerian ocean-physics simulations (Durran, 2010, Blazek, 2015). The hydrodynamic data are embedded on a 2D grid, where data attribute values are organised in arrays with one attribute array per grid cell. This means each valid grid cell located within the ocean contains a set of attributes, whereas landmass cells are either excluded from the grid or represented by attribute filling values (e.g. zero flow). The key attributes of this study are as follows:

- Zonal and meridional velocity (2D vector): $V = (u, v)$
- Velocity magnitude, i.e. *speed* (real, positive, scalar): $|V|$
- Velocity direction, i.e. *angular direction* (real, circular, scalar): θ_V
- Flow divergence (real, divergent, scalar): $\nabla \cdot V$
- Bathymetric depth (real, positive, scalar): z_{depth}
- Sea surface temperature (real, divergent, scalar): SST

The physical attributes of *water density* and *sea-surface salinity* were also considered, yet they express insufficient variability in the target area of the experiment and are thus excluded from the mapping consideration.

3.2 Ocean visualisation via contour-based CoD

In contrast to CoD for coastal data (Semmo et al., 2013), our interest is not limited to shoreline distance contours. However, our flow-feature line tracing is equally based on attribute isocontouring. These contours are represented by individual polyline segments that give access to the following *visual channels* in the mapping stage, as illustrated by fig. 2:

- **Stroke position** X_s: contour corner positions based on the isocontouring of an attribute function $f(Y = y)$, with y being the threshold value.

- **Stroke length** l_s: length of stroke(s) between two corners $(x_1, x_2) \in X_s$, where $l_s = 1$ results in a straight solid line.
- **Stroke spacing** Δd_s: spacing of strokes between two corners $(x_1, x_2) \in X_s$, which only applies if $l_s < 1$.
- **Stroke width** w_s: line width of a contour stroke.
- **Stroke margin** Δw_s: lateral spacing between parallel contour lines when isocontouring multiple values of $f(Y)$. This attribute is represented by the *contour density*, and governed by the chosen isovalues.

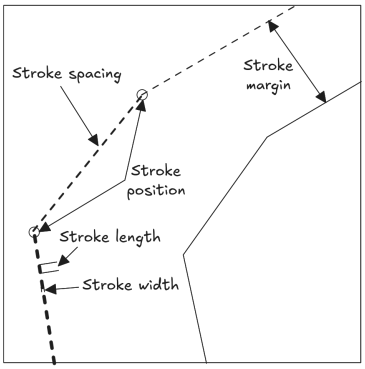

Figure 2. Visual channels related to contour strokes.

Although contour dots can already be generated within this set of channels (i.e. $l_s = w_s \ll \Delta d_s$), nautical maps can also include randomly distributed point indicators that are spaced anisotropically and at metric distances, as shown in fig. 1. The metric basis of these features facilitates direct distance measurements between any set of points on the map. This cartographic feature is integrated through a discrete scatter plot, giving access to the visual channel of point density ρ_p.

Historical nautical maps do not have a coloured ocean background due to the prohibitive expense of colour printing in the past. Yet, modern digital maps can tone-map the ocean background in several ways, including (a) a constant, thematic marine colour-tone, (b) a (tone-mapped) bathymetry profile, (c) a thematically-patterned texture (such as a parchment patina), or (d) an attribute-related colour mapping. This colour mapping is further integrated with the cartographic style to facilitate the modulation of the following visual channels.

- **Foreground colour tone** $C(x,y)$: colour hue (monochromatic) or hues (multichromatic) of the colour map.
- **Foreground colour intensity** $I(x,y)$: for achromatic colour maps, this is the fraction of foreground colour plotted on top of the background; for mono- or multichromatic colour maps, it is the colour brightness.
- **Foreground colour opacity** $\alpha(x,y)$: the intermixing fraction between upper-layer foreground colour and lower-layer background colour.

Bézier curve tapering of fluid hatches and tufts The presented contour stroke or point markers are non-orientable. Even though it is possible to orient the contour strokes in different directions, this is an inadequate approach as it removes the line continuity necessary to perceive the strokes as part of a contour. We propose to also scatter individual line segments (i.e. *hatches*, see fig. 3(a)) across the fluid domain. In order to distinguish hatches from contour lines, the hatches are drawn as tapered Bézier curves. Beyond improved hatch orientability, the Bézier tapering adds to the perception of hand-drawn line aesthetics. The Bézier hatches give access to the following interchangeable or independent visual channels:

- **Hatch position** X_H: sampled start positions $x \in X_H$ per hatch stroke.
- **Hatch density** ρ_H: fraction of pixels covered by hatches relative to total pixel number in a given area.
- **Hatch orientation** θ_H: angular bearing of a hatch stroke between its start and end-point anchors, $\theta_H = 0$ pointing directly North. The angle follows a clockwise orientation.
- **Hatch length** l_H: stroke length of individual hatches.
- **Hatch width** w_H: line width of a hatch stroke.

One drawback of lines and curves as orientation indicators is the absence of a defined start or end-point for each indicator. This absence not only makes it difficult to accurately localise markers, but also creates an ambiguity between complementary angles (e.g. differentiating between 0° and 180°). Traditionally, this is addressed through the use of arrows. However, arrow markers suffer from scaling and occlusion issues, meaning that wider arrow stems require an exponentially-larger tip, and that the tips frequently occlude other data items, as illustrated by (Kehl et al., 2022), fig. 4a. Therefore, our cartographic style uses *tufts* to disambiguate orientation markers. Tufts, as shown in fig. 3(b), are common orientation indicators in aerodynamic visualisation, as demonstrated by (Post and Van Walsum, 1993), and seamlessly combine point and hatch markers for spatially-distributed attribute mapping with minimal clutter-related occlusions. They also combine the channel modulations of both the point and hatch markers.

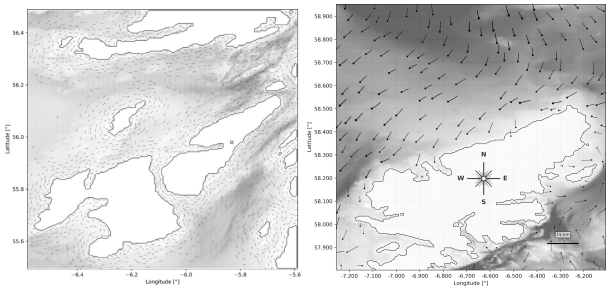

(a) (b)

Figure 3. Visual comparison between hatches (a) and tufts (b) as orientable stroke glyphs.

Geographic heading via auto-positioned compass rose Grid lines and circular graphics are common background elements of cartographic maps to indicate the scale and orientation of the plot (as represented in fig. 1). A classic circular indicator is the compass rose, which we adopted for this new cartographic style. In order to avoid data occlusion from the compass-rose, the visualisation algorithm needs to determine a non-occlusive position and scale for the indicator on the map. We decide to place the compass rose on land areas present in the plot, as our visualisation-specific target is the hydrological domain. The placement and scaling are performed according to algorithm 1. An example of compass rose placement and related grid line plots is shown in fig. 4.

4. Visual encoding experiments around the Hebrides

The presented approach is evaluated for the oceanographic setting of the Hebrides island chain, Scotland, UK. This case study

This contribution has been peer-reviewed. The double-blind peer-review was conducted on the basis of the full paper.
https://doi.org/10.5194/isprs-annals-XI-4-2026-221-2026 | © Author(s) 2026. CC BY 4.0 License.

Algorithm 1: Compass-rose position and scaling algorithm

Result: Pixel centre position p_{xy} and pixel radius r of the target compass rose bitmap

Compute signed distance function $D(p_1, p_2)$ to shore;
Mask M_{land}: $M_{\text{land}}(x,y) = 1 \mid D(p_{(x,y)}, p_{\text{shore}}) > 0$;
Erode M_{land} binary field using a 3×3 disk-kernel;
Split connected-components of $M_{\text{land}} \rightarrow C_i \; \forall \; i = \{0..n\}$;
Sort C_i so that area $A(C_0) \rightarrow max(A(C_i)) \; \forall \; i = \{0..n\}$;
Get centroid $c(C_0) = p_{xy} \rightarrow$ circumcircle centre of C_0;
Compute radius r by lookup in $D(p_{xy}, p_{\text{shore}})$;

Figure 4. Example plot of compass rose and grid lines, embedded in a contour-plot of V with a parchment patina.

was chosen due to the presence of coastlines, offshore turbulent eddies, as well as the open ocean in the region, providing views on multiple scales.

Through a qualitative assessment approach, the study addresses *which visual encodings between hydrodynamic attributes and visual channels perform well for different visual-cognitive tasks*. The quality criteria, which relate to individual cognitive tasks, are adopted from the *PREVis Perceived Readability Score* (Cabouat et al., 2025). The criteria and scoring scales are shown in the PREVis online questionnaire[2] (see fig. 5), as presented in appendix B and the supplementary material.

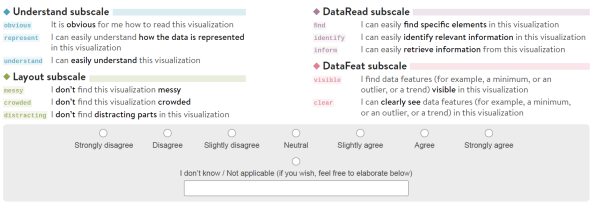

Figure 5. PREVis criteria with score description and scale.

4.1 Hydrological setting of the Hebrides

The Hebrides are located on the most north-western corner of Scotland. A channel, 21 km to 44 km wide with a dominant southward current, separates the island chain from the mainland, as visible in fig. 6. The ocean around the island chain is turbulent, containing several eddying gyres of around 25 km in diameter. The eastward gyres in the channel between the mainland are predominantly rotating counter-clockwise, whereas gyres south and north-east of the islands rotate clockwise. The Hebrides are in the transition zone between the sea climate of the British Isles and the sub-polar climate of the open-ocean North Atlantic. This climatological variability manifests in physical attributes such as sea-surface temperature, sea-surface salinity, and overall current velocity magnitude.

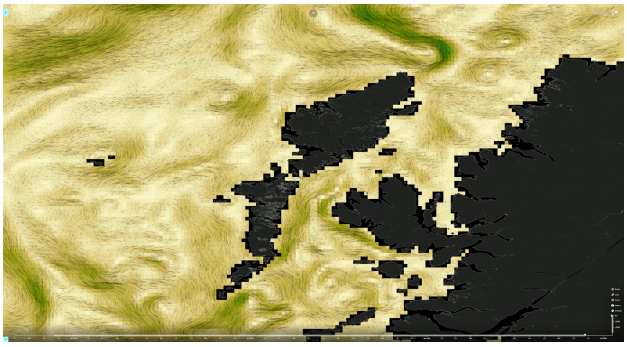

Figure 6. Hydrological setting of the Hebrides, illustrated via the Copernicus Data Marine Systems[3], using a particle tracer plot on the seawater velocity.

4.2 Experiment dataset and procedure

The study uses the Atlantic European North-West Shelf Ocean Physics Analysis & Forecast dataset (European Union-Copernicus Marine Service, 2018) with the attributes outlined in section 3.1. The grid of the hydrodynamic field is defined on a $1/36° = 0.027°$ grid scale ($\simeq 1.73 - 2.77km$), covering the area of 16°W to 10°E and 46°N to 61.3°N. The value discretisation uses a regular rectangular grid type with 936 longitudinal and 551 latitudinal data points. All experiments use the data captured for the 1st January 2022.

The GEBCO digital elevation model (DEM) by (Weatherall et al., 2015) is used for elevation data to encode bathymetric depth and to determine coastal distances on the grid. This DEM operates at a higher lateral resolution of 15 arcseconds $= 0.0042°$ per grid cell. In terms of processing, this grid resolution difference has no impact, as we are concerned with individual attributes. However, the resolution discrepancy is visible in the resulting figure because landmasses are plotted on top of the hydrodynamic data. Consequently, flow patterns close to the shoreline are occluded by the landmass.

The experiment is split into two parts. Part A follows a common *design space exploration* approach (Card and Mackinlay, 1997), randomly modulating the mapping of data attributes (given in section 3.1) to visual channels, focusing on 53 individual cases that represent unique, suitable data-channel pairs (see table 1). Part B compares perceived readability of existing visualisation techniques, such as multi-panel or the perceptual visualisation, with the cartographic visualisation approach outlined above. For this approach, an expert selection resulted in six different mappings of the hatch markers, each with different numbers of mapped attributes. When co-visualising five different attributes, two competing visual designs are shown and compared. Part A is done by individual user judgement, whereas Part B covers a user study of three participants. Both parts score the individual visualisations according to the PREVis scale (see fig. 5).

[2] PREVis Perceived Readability Evaluation in Visualization – `https://aviz.fr/PREVis/`

[3] Copernicus Marine Data Store - `https://data.marine.copernicus.eu/products`

Technique	Channel	Attribute
Tufts & hatches	Orientation θ_H	velocity $V=(u,v)$
	Position X_H	SST, $\lvert V\rvert$, $\nabla\cdot V$, z_{depth}
	Density ρ_H	SST, $\lvert V\rvert$, $\nabla\cdot V$, z_{depth}
	Length l_H	SST, $\lvert V\rvert$, $\nabla\cdot V$, z_{depth}
	Width w_H	SST, $\lvert V\rvert$, $\nabla\cdot V$, z_{depth}
Contour strokes	Position X_s	SST, $\lvert V\rvert$, $\nabla\cdot V$, z_{depth}
	Pattern $f(l_s,\Delta d_s)$	SST, $\lvert V\rvert$, $\nabla\cdot V$, z_{depth}
	Width w_s	SST, $\lvert V\rvert$, $\nabla\cdot V$, z_{depth}
	Margin Δw_s	unused
Background	Colour map	SST, $\lvert V\rvert$, $\nabla\cdot V$, z_{depth}

Table 1. Mapping of visual channels to hydrodynamic attributes within the experiment part A. For simplicity, the stroke parameters l_s and Δd_s are combined into the channel of *stroke pattern* $f(l_s,\Delta d_s)$.

4.3 Experiment results

Part A of the user study is scored by the lead author. Table 2 lists the aggregate scores over the 53 individual cases, grouped by the number of mapped channels.

#	Understand	DataRead	Layout	DataFeat	Total
2	*21*	*21*	*21*	*10*	**73**
3	*21*	15	*21*	4	61
4	19	13	9	19	60
5	15	7	6	15	43

Table 2. Average PREVis perceived readability score for varying number of encoded attributes (denoted as ‘#’). The highest possible scores per category are: Understand: 21; Layout: 21; DataRead: 21; DataFeat: 14; Total: 77. Top scores per category are emphasised in italics, whereas the total top-score is highlighted in bold.

Selected example visualisations are shown in fig. 7, fig. 8 and fig. 9, demonstrating the breadth of possible visual encodings. Results in table 2 show an inverse correlation between the number of encoded attributes and the readability score, indicating that more complex visualisations reduce visual comprehension. In detail, visual *understanding* remains high for up to four attributes, while sharply decreasing afterwards. The capacity to *read the data* through the visualisation decreases steadily with increasing attribute counts. The *layout* is excellent for up to three co-visualised attributes, dropping sharply beyond that point. Yet, the potential to *see* and *comprehend* data features and trends improves with an increased number of mapped attributes.

Part B compares established visualisation techniques with the presented cartographic styles in an online survey that is completed by all three authors. The results in table 3 present the average PREVis scores across all participants per visualisation approach.

As shown in table 3, established methods score well in the *Understand* category. In more detail, we see that these methods are decisively more *obvious* to read and *represent* the data more accessibly. They are also less *messy*, less *crowded* and less *distracting*. Data features are perceived as more *visible* in quiver plots, colour maps and multi-panel frames than in cartographic plots. In contrast, cartography-based designs perform well in terms of *data reading*. Green-coloured CoD visualisations in table 3 match or exceed average scores of established techniques for *finding* and *identifying* individual data items and their

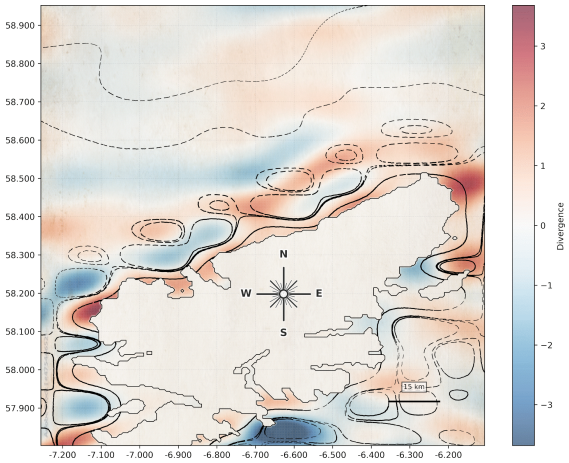

Figure 7. Contour stroke visualisation, 4 visual encodings: $SST \rightarrow X_s$, $|V| \rightarrow f(l_s,\Delta d_s)$, $z_{\text{depth}} \rightarrow w_s$, $\nabla\cdot V \rightarrow C(x,y)$.

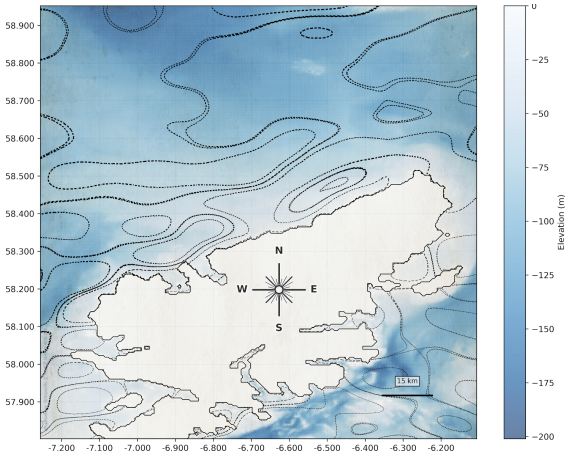

Figure 8. Contour stroke visualisation, 4 visual encodings: $\nabla\cdot V \rightarrow X_s$, $SST \rightarrow f(l_s,\Delta d_s)$, $|V| \rightarrow w_s$, $z_{\text{depth}} \rightarrow C(x,y)$.

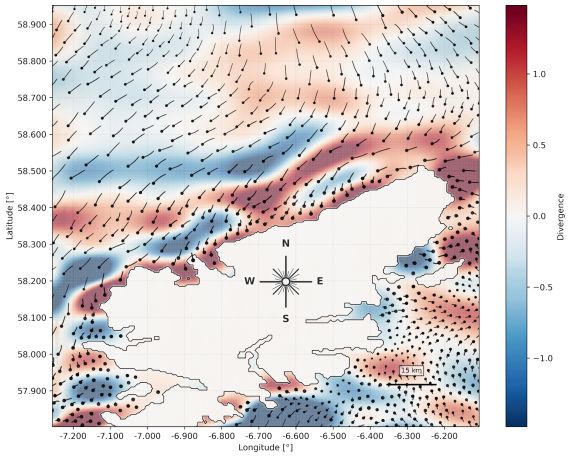

Figure 9. Tuft visualisation, 5 visual encodings: $SST \rightarrow \rho_H$, $V \rightarrow \theta_H$, $|V| \rightarrow l_H$, $z_{\text{depth}} \rightarrow w_H$, $\nabla\cdot V \rightarrow C(x,y)$.

Category	Quiver-Plot	Perceptual Colourmap	Multi-Panel	Hatch: 1 Channel	Hatch: 2 Channels	Hatch: 3 Channels	Hatch: 4 Channels	1st Hatch: 5 Channels	2nd Hatch: 5 Channels
Obviousness	6.3	5.3	6.0	4.7	4.3	4.3	4.3	4.3	4.3
Representation	5.0	4.7	6.7	6.3	3.7	4.3	3.7	4.0	4.0
Understanding	4.7	3.0	5.7	3.0	3.0	4.7	5.0	5.3	3.7
Find	6.0	4.3	5.3	4.0	2.7	4.7	6.3	6.0	4.7
Identify	5.0	3.7	5.7	3.3	3.0	4.7	6.0	5.3	5.0
Inform	3.7	2.7	5.3	2.3	3.3	4.7	4.7	4.7	3.7
Messy	6.0	5.0	4.0	4.7	4.7	4.3	3.3	2.7	3.3
Crowded	6.0	5.7	4.0	5.0	5.3	4.7	4.0	2.7	3.7
Distract	6.7	5.7	4.7	5.7	4.7	4.3	4.3	3.5	3.0
Features Visible	4.7	5.3	5.3	5.0	3.7	4.3	5.0	4.3	4.3
Features Clear	5.7	5.0	5.3	4.3	3.3	5.3	5.3	5.0	3.7
Understand	5.3	4.3	6.1	4.7	3.7	4.4	4.3	4.6	4.0
DataRead	4.9	3.6	5.4	3.2	3.0	4.7	5.7	5.3	4.4
Layout	6.2	5.4	4.2	5.1	4.9	4.4	3.9	2.9	3.3
DataFeat	5.2	5.2	5.3	4.7	3.5	4.8	5.2	4.7	4.0
Total	**21.6**	18.5	**21**.0	17.7	15.1	18.3	**19.1**	17.5	15.7

Table 3. Average PREVis perceived readability score, comparing different visualisation approaches with one another. Colours highlight top-scores in categories favouring established techniques (blue) or the cartographic design (teal), or where the new cartographic design is at least on a similar level to established techniques (lime-green).

correlation, particularly when using a high number of visual channels. These examples also retain *clear* and *visible* perception of overall trends (see green marker within *DataFeat* category in table 3), despite conveying large amounts of information.

When comparing hatching-styled cartographic visualisations with one another (table 3, column 5–10), the presence of more visual channels conveys a greater amount of information, though this comes at the cost of aesthetics, visible in decreasing scores for the *layout* category. The two competing five-attribute designs score differently, particularly in terms of *data-reading* tasks.

5. Discussion

This section aggregates the results of both user studies for a conclusive interpretation of study outcomes. The remarks further address the guiding research question. Lastly, the results are aggregated into some key insights on the presented cartographic technique, the visual mapping of the data and the reliability of the chosen perceived readability score of PREVis.

5.1 Experiment interpretation

The observed PREVis scores in Part A support the argument that increasingly complex visual encodings hinder perceived readability, and thus the comprehension of hydrological patterns and trends. Yet, this statement is not entirely reliable and requires future refinement, due to the individual participant within the experiment. Part B shows that the chosen style of the visualisation impacts perceived readability for the audience. This second experiment remedies the limited reliability of previous results through expanded participation and by including more domain expertise. A larger user study involving a more diverse audience (including hydrology domain-experts) is facilitated through a replicable online-survey format designed around the PREVis evaluation and specified directly for evaluation of ocean-flow hydrodynamic patterns. We plan to use this format for repeated, expanded user studies with different audiences in the future.

In more detail, the more obvious data representation and improved feature visibility of traditional methods could simply be related to audience familiarity with these plot types, though the gaps to the cartographic design scores are too large to be exclusively attributed to *familiarity*. The difference in layout scores could be due to the fewer co-attributes being shown, though the multi-panel with many attributes also outperforms the cartographic design results. The high scores in data understanding and reading for the five-attribute cartographic design shows that with a careful visual mapping of data to visual channels, the cartographic design approach can be a highly informative style of visual information communication. This hypothesis is further supported when considering the direct comparison between the two five-attribute visualisations (table 3, columns 9 and 10).

In terms of the research question *which visual encodings of hydrodynamic data to visual channels perform well for visual-cognitive tasks*, the PREVis experiment shows that the most effective visualisation remains the quiver plot, mapping flow direction and flow magnitude to arrow bearing and length. The second best result is the multi-panel visualisation, mapping flow vectors to arrow glyphs and flow magnitude, flow divergence and temperature to (adequate) colour maps. Yet, both results are affected by familiarity bias. A cartographic hatching design mapping four attributes - with flow direction to hatch orientation, temperature to hatch density, flow speed to hatch length and bathymetry to achromatic intensity - performs third-best overall and best among the cartographic designs.

Considering the hydrological insight, we can deduce from fig. 7 that areas of negative flow divergence (i.e. flow sinks) coincide with areas of high temperature. This supports the geophysical hypothesis of warm eddies attracting water masses as net flow receivers. Generally, the encoding of divergence via density, contour position (fig. 8) or divergent background colour (fig. 7) is advantageous for locating gyres and similar coherent flow structures.

5.2 Insights for visualisation practice in oceanography

From the user study responses and their interpretation, as well as by revising the generated design space in experiment part A, we identify three major insights that are shared in this context.

This contribution has been peer-reviewed. The double-blind peer-review was conducted on the basis of the full paper.
https://doi.org/10.5194/isprs-annals-XI-4-2026-221-2026 | © Author(s) 2026. CC BY 4.0 License.

First of all, simple mappings and low-dimensional data representations, through the use of straight arrow glyphs or colour maps, are still preferred or beneficial for diverse audiences without a specific background and training. Visual familiarity plays a role, yet results indicate that new visual designs should exceed a mental threshold before being considered a viable alternative. Secondly, study participants prefered multi-panel visualisations, with anecdotal feedback suggesting that they would retain a multi-panel setup while embedding cartographic subplots. However, this statement is conditional on the ability of digital zooming. Lastly, alongside the central design elements of visualisation, legends and scale-bars become increasingly important the more attributes are mapped, because the design space gets more complex and each used visual channel becomes less prominent. One challenge here is the representation of visual channels that are rarely used and thus not available in plotting interfaces (e.g. matplotlib). Proxy representations for legends need to be found for these cases. Moreover, data that are mapped to less effective visual channels require more stringent binning to facilitate their visual distinction in the composed plot.

5.3 Future extensions & research

The presented CoD technique is a good starting point for visually encoding multivariate, hydrodynamic field datasets into unique visual channels that facilitate ample customisation. Extended features, such as the tuft-enhanced scatter plots, the compass rose and the parchment patina, are aesthetically pleasing and fit the cartographic theme of the intended visual style. The colour mapping can be improved by separating tone, intensity, and opacity. Such separation is exemplified by the perceptual colour maps within the literature (Kehl et al., 2022). On the technical side, the implemented technique can be extended to time-varying data through animations, while also addressing performance-related bottlenecks. Current investigation aims to integrate the technique with bathytopographic surfaces in 3D coordinate space (see fig. 10).

A major downside of the presented work is the limited sample size in the evaluation and user study. The PREVis criteria and the scoring system are adequate for the intended evaluation purpose. The framework delivers quantitative measurements on the perceived readability of the visualisation. Yet, a user study with more participants covering a wider range of professional backgrounds, expertise and domain-specific knowledge is required to reliably estimate the technique's applicability for its intended practical application. Moreover, the comparison of single-panel and multi-panel visualisations requires further investigation to estimate the trade-off between visual complexity within a single view and the relatability of visual relationships between multiple panels, as initially discussed in the related literature (Javed and Elmqvist, 2012).

6. Conclusions

This paper presents a re-interpretation of the water-lining cartographic-oriented design by (Semmo et al., 2013), extended for the multivariate attribute visualisation of hydrodynamic ocean physics field datasets. The visualisation technique disentangles visual channels of contour strokes, scatter plots, hatches & tufts and plot background, and facilitates their individual modulation through the mapping of physical attributes. Thematic map elements, such as a scale-bar and a compass-rose, are added to the visual composition.

The resulting visualisation technique is evaluated on a hydrodynamic case study around the Hebrides island chain in Scotland, UK. The evaluation is split into two different experiments: part A evaluates 53 uniquely-created visualisations with respect to the PREVis perceived readability method; part B compares the cartographic style with established visualisation techniques in a small user study. Both studies indicate overall that participants prefer established visualisation techniques and score those generally better than cartographic visualisations. Yet, some higher-complexity cartographic plots (e.g. with four and five attributes) receive scores comparable to established techniques. The new visual design performs particularly well in data understanding and reading. Building on the early results, the user study shall continue with a more diverse audience to provide reliable statements on the effectiveness of the visual communication approach. Extending the visualisation style to 3D coordinate space while addressing performance bottlenecks are key future objectives.

Software availability

The presented methods are implemented in Python scripts to generate the demonstrated plots, given that the input data are formatted as defined in (European Union-Copernicus Marine Service, 2018). The scripts can be obtained via Github: `https://github.com/RUG-VIS/ocean_cartographic-visual-design`. The project is distributed under the *Lesser Gnu Project Licence (LGPL) 2.1*.

Acknowledgements

This manuscript is an extension of the B.Sc. thesis entitled *Exploring the Visual Design Space of 2D Eulerian Fluid Flow Visualizations* by Brad W. Robertson. The authors thank the constructive input from the workshop participants of the OceanParcels 10-year anniversary event[4]. This study has been conducted using E.U. Copernicus Marine Service Information. The user study survey was performed using *SurveyMonkey*[5].

A. Visual channel ranges in CoD implementation

- **Stroke position** X_s: [lon, lat] limits of the study area
- **Dash length** ds: $\{1..25\}$ (downscaled to area extent)
- **Stroke length** : **Stroke spacing** ratio: $0.6 * l_s + 0.4 * \Delta d_s$
- **Stroke width** w_s: $\{0.3..2.0\}$ pt.
- **Stroke margin** Δw_s: $\frac{1}{6}$ of contoured attribute range

- **Foreground colour tone** $C(x,y)$: RGB triplet range $(\{0..255\},\{0..255\},\{0..255\})$
- **Foreground colour intensity** $I(x,y)$: $(1-i)$ white $+$ i black, with $i = \{0..1\}$
- **Foreground colour opacity** $\alpha(x,y)$: $(1-\alpha)$ background $+\,\alpha$ foreground, with $\alpha = \{0..1\}$

- $|\text{lon}| = \text{lon}_{max} - \text{lon}_{min}$, $|\text{lat}| = \text{lat}_{max} - \text{lat}_{min}$
- **Hatch position** X_H: [lon, lat] limits of the study area
- **Hatch density** ρ_H: $0.1\ \frac{\Delta\text{lon}+\Delta\text{lat}}{2}\ \frac{0.02}{|\text{lon}|+|\text{lat}|}$
- **Hatch orientation** θ_H: $\{-\pi..+\pi\}$
- **Hatch length** l_H: $\{0..l_{H_{max}}\}$, $l_{H_{max}} = \frac{|\text{lon}|+|\text{lat}|}{40}$
- **Hatch width** w_H: $\{0.5..1.5\}$ pt.

[4] Parcels 10-year anniversary event - `https://parcels-code.org/blog/10year-event`
[5] SurveyMonkey - `https://surveymonkey.com`

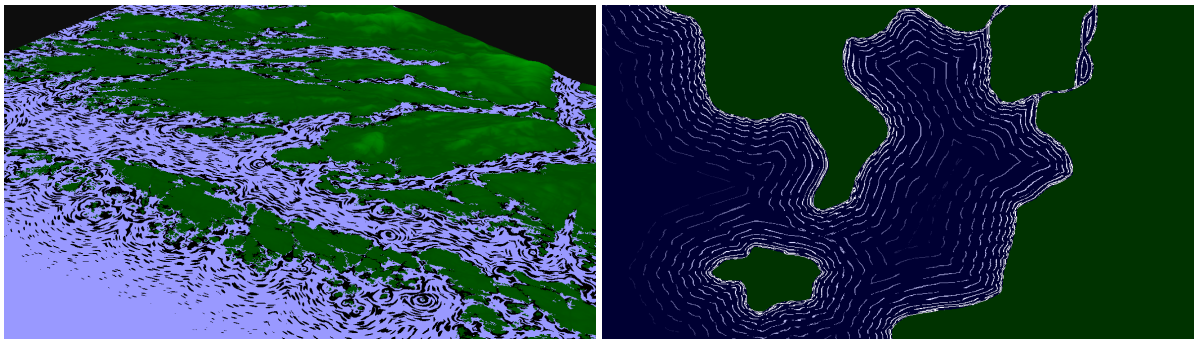

(a) (b)

Figure 10. Prototypes of real-time rendered CoD (Semmo et al., 2013), for DEMs of the Norwegian Atlantic coastline. These are student project results of the Geo-Visualization course (University of Groningen) 2024(a) & 2025(b).

B. PREVis scale explanation

B.1 *Understand* scale

`obvious`: It is **obvious** for me how to read this visualization.

- Can you distinguish different hydrodynamic attributes ?
- Can you distinguish ocean- & terrestrial elements ?
- Can you geographically locate the area ?

`represent`: I can easily understand **how the data is represented** in this visualisation.

- Can you tell which attribute is represented by which symbol(s) or colour map (i.e. visual channel) ?
- Can you identify the baseline (i.e. zero-point) of the attribute from the symbol(s) or colour map ?

`understand`: I can **easily understand** this visualisation.
Details: expected insight _just from the visuals (i.e. how many features can you easily identify ?):

- The water at the northern coastline of island flows towards the coastline
- The water at the southern coastline of island flows away from the coastline
- The ocean around the island has a turbulent, non-laminar flow, meaning: the flow direction varies visibly and it has no obvious general flow direction
- The eddies are areas with 0 m/s velocity at the centre, and a divergence of 0 m/s at its boundary
- Flow direction, divergence and eddy-location are correlated
- In the Irish Sea, between the mainland and the island, there are several smaller eddies
- There are 2 clockwise- and 1 counter-clockwise turning eddies north of the island
- The winding of eddies south of the island varies – some turn clockwise, some turn counter-clockwise
- The seawater temperature at the coast differs from than in the (northerly) open ocean
- There is a deep ocean trench off the south-southeast center shoreline of the island

B.2 *DataRead* scale

`find`: I can easily **find specific elements** in this visualisation.

- Can you locate areas of fast-/slow-flowing water ?
- Can you locate areas of calm, nearly-steady waters ?
- Can you locate ocean trenches- and ridges ?

`identify`: I can easily **identify relevant information** in this visualisation.

- Can you identify & distinguish areas of fast-flowing water from areas with slow-flowing water ?
- Can you identify & distinguish areas of equal flow direction from areas with a different flow direction ?
- Can you distinguish between warm and cold water areas ?
- Can you distinguish between deep and shallow waters ?

`information`: I can easily **retrieve information** from this visualisation.

- Can you directly approximate the flow velocity (in [m/s]) in the visualisation ?
- Can you directly read- or approximate the seabed elevation (i.e. bathymetry; in [m]) from the visualisation ?
- Can you infer the ocean water temperature (in [$^{\circ}C$]) from the visualisation?

B.3 *Layout* scale

`messy`: I **don’t** find this visualisation **messy**.

- Can you focus on individual visual elements in the visualisation ?
- Can you distinguish *lines* from *points* ?
- Can you see the background even in densely-sampled areas ?
- Can you identify all colours separately, or do you get the impression that there are duplicate colours due to colour deficiencies ?

`crowded`: I **don’t** find this visualisation **crowded**.

- Do you perceive a lot of *occlusions* in the visualisation ?
- Do you perceive the visualisation to *be nervous* ?

`distract`: I **don’t** find **distracting parts** in this visualisation.

- Are there graphical elements that have nothing to do with the data, the scale or the orientation ?
- If the visualisation uses saturation, brightness and/or transparency together: are there discrepancies between the overlay, the data scale and the background colour ?

B.4 *DataFeat* scale

`visible`: I *perceive* data features (for example, a minimum, or an outlier, or a trend) to **be visible** in this visualisation (i.e. they are *visibly existent*).

`see`: I can **see** data features (for example, a minimum, or an outlier, or a trend) **clearly** in this visualisation (i.e. they are *distinct* from their surroundings).

References

Arakawa, A., Lamb, V. R., 1977. Computational Design of the Basic Dynamical Processes of the UCLA General Circulation Model. *Methods in Computational Physics: Advances in Research and Applications*, 17, 173–265.

Blazek, J., 2015. *Computational Fluid Dynamics: Principles and Applications*. 3rd edn, Butterworth-Heinemann.

Cabouat, A.-F., He, T., Isenberg, P., Isenberg, T., 2025. PREVis: Perceived Readability Evaluation for Visualizations. *IEEE Transactions on Visualization and Computer Graphics*, 31(1), 1083–1093. https://doi.org/10.1109/tvcg.2024.3456318.

Card, S., Mackinlay, J., 1997. The structure of the information visualization design space. *Proceedings of VIZ ’97: Visualization Conference, Information Visualization Symposium and Parallel Rendering Symposium*, 92–99.

Chi, E., 2000. A taxonomy of visualization techniques using the data state reference model. *IEEE Symposium on Information Visualization 2000. INFOVIS 2000. Proceedings*, 69–75.

Durran, D. R., 2010. *Numerical Methods for Fluid Dynamics: With Applications to Geophysics*. 32, Springer Science & Business Media.

European Union-Copernicus Marine Service, 2018. Atlantic - european north west shelf - ocean physics analysis and forecast.

Fauville, G., Voşki, A., Mado, M., Bailenson, J. N., Lantz-Andersson, A., 2024. Underwater virtual reality for marine education and ocean literacy: technological and psychological potentials. *Environmental Education Research*, 0(0), 1–25. https://doi.org/10.1080/13504622.2024.2326446.

Gutierrez, D., Seron, F. J., Munoz, A., Anson, O., 2008. Visualizing Underwater Ocean Optics. *Computer Graphics Forum*, 27(2), 547-556. https://doi.org/10.1111/j.1467-8659.2008.01152.x.

Häberling, C., Bär, H., Hurni, L., 2008. Proposed Cartographic Design Principles for 3D Maps: A Contribution to an Extended Cartographic Theory. *Cartographica*, 43(3), 175-188. https://doi.org/10.3138/carto.43.3.175.

Haller, G., Poje, A., 1998. Finite time transport in aperiodic flows. *Physica D: Nonlinear Phenomena*, 119(3), 352-380. https://doi.org/10.1016/S0167-2789(98)00091-8.

Hunter, J. D., 2007. Matplotlib: A 2D graphics environment. *IEEE Annals of the History of Computing*, 9(03), 90–95.

Javed, W., Elmqvist, N., 2012. Exploring the design space of composite visualization. *2012 IEEE Pacific Visualization Symposium*, 1–8.

Kehl, C., Fischer, R. P. B., van Sebille, E., 2021. Practices, pitfalls and guidelines in visualising Lagrangian ocean analyses. *ISPRS Annals of the Photogrammetry, Remote Sensing and Spatial Information Sciences*, V-4-2021, 217–224. https://doi.org/10.5194/isprs-annals-V-4-2021-217-2021.

Kehl, C., Lobelle, D. M. A., van Sebille, E., 2022. Perceptual multivariate visualisation of volumetric Lagrangian fluid-flow processes. *Frontiers in Environmental Science*, 10. https://doi.org/10.3389/fenvs.2022.941910.

Masse, A., Christophe, S., 2015. Homogeneous geovisualization of coastal areas from heterogeneous spatio-temporal data. *The International Archives of the Photogrammetry, Remote Sensing and Spatial Information Sciences*, 40, 509–516. https://doi.org/10.5194/isprsarchives-XL-3-W3-509-2015.

Masse, A., Christophe, S., 2016. Améliorer la perception du réalisme dans la géovisualisation du littoral. *Revue Internationale de Géomatique (RIG)*, 26(4), 403–424. https://doi.org/10.3166/rig.2016.00008.

Medyńska-Gulij, B., 2022. Geomedia Attributes for Perspective Visualization of Relief for Historical Non-Cartometric Water-Colored Topographic Maps. *ISPRS International Journal of Geo-Information*, 11(11). https://doi.org/10.3390/ijgi11110554.

Munzner, T., 2009. A Nested Model for Visualization Design and Validation. *IEEE Transactions on Visualization and Computer Graphics*, 15(6), 921-928. https://doi.org/10.1109/TVCG.2009.111.

Munzner, T., 2014. *Visualization Analysis and Design*. AK Peters & CRC Press.

Post, F. H., Van Walsum, T., 1993. Fluid flow visualization. *Focus on Scientific Visualization*, Springer, 1–40.

Semmo, A., Kyprianidis, J.-E., Trapp, M., Döllner, J., 2013. Real-time rendering of water surfaces with cartography-oriented design. *Proceedings of the Symposium on Computational Aesthetics (CAE ’13)*, ACM, 5–14.

Semmo, A., Trapp, M., Jobst, M., Döllner, J., 2015. Cartography-Oriented Design of 3D Geospatial Information Visualization – Overview and Techniques. *The Cartographic Journal*, 52(2), 95–106. https://doi.org/10.1080/00087041.2015.1119462.

Shadden, S. C., Lekien, F., Marsden, J. E., 2005. *Definition and properties of Lagrangian coherent structures from finite-time Lyapunov exponents in two-dimensional aperiodic flows*. 212.

Shi, J., Zhu, D., Zhang, Y., Wang, Z., 2012. Realistically rendering polluted water. *The Visual Computer*, 28(6), 647–656. https://doi.org/10.1007/s00371-012-0685-0.

Steenbeek, J., Felinto, D., Pan, M., Buszowski, J., Christensen, V., 2021. Using Gaming Technology to Explore and Visualize Management Impacts on Marine Ecosystems. *Frontiers in Marine Science*, Volume 8 - 2021. https://doi.org/10.3389/fmars.2021.619541.

Trapp, M., Semmo, A., Döllner, J., 2015. Interactive rendering and stylization of transportation networks using distance fields. *GRAPP*, 207–219.

Van Wijk, J. J., 2002. Image based flow visualization. *Proceedings of the 29th annual conference on Computer graphics and interactive techniques*, 745–754.

Weatherall, P., Marks, K. M., Jakobsson, M., Schmitt, T., Tani, S., Arndt, J. E., Rovere, M., Chayes, D., Ferrini, V., Wigley, R., 2015. A new digital bathymetric model of the world’s oceans. *Earth and Space Science*, 2(8), 331-345. https://doi.org/10.1002/2015EA000107.

Zhang, S., Zhang, T., Wu, Y., Yi, Y., 2016. Flow simulation and visualization in a three-dimensional shipping information system. *Advances in Engineering Software*, 96, 29-37. https://doi.org/10.1016/j.advengsoft.2016.01.004.